ELSEVIER

Journal of Power Sources 54 (1995) 406–410

JOURNAL OF POWER SOURCES

Formation of the ω-type phase by lithium intercalation in (Mo, V) oxides deriving from V_2O_5

C. Delmas, H. Cognac-Auradou

Laboratoire de Chimie du Solide du CNRS and Ecole Nationale Supérieure de Chimie et Physique de Bordeaux, Université Bordeaux I, 33405 Talence Cedex, France

Abstract

Large amounts of lithium have been intercalated electrochemically and chemically in molybdenum-substituted V_2O_5-deriving phases like the $Mo_yV_{2-y}O_5$ solid solution ($0 \leqslant y \leqslant 0.60$) and $Mo_6V_9O_{40}$ ($Mo_{0.8}V_{1.2}O_{5.33}$). In all cases, the ω-type phase is irreversibly formed in the $Li_3Mo_yV_{2-y}O_5$ and $Li_3Mo_{0.8}V_{1.2}O_{5.33}$ compositions. Like in the case of pure V_2O_5, these new materials exhibit very good cycling properties in lithium batteries. Depending on the amount of molybdenum and the potential domain, the specific energy lies in the 900–500 Wh/kg range. The ω-type phases present a rocksalt-type structure with all cations statistically distributed among the octahedral sites, the general formula being $Li_x\square_{0.60-x}Mo_vV_{0.40-v}O$ ($v = y/5$) or $Li_x\square_{0.625-x}Mo_{0.150}V_{0.225}O$ depending on the starting material. When such materials are formed, for the first time, from V_2O_5-related phases, they exhibit a superstructure with a tetragonal unit cell. Due to the destabilization of the rocksalt-type lattice for the highest amount of vacancies, the cell voltage increases very rapidly at the end of charge and, therefore, it is impossible to remove the last lithium atoms.

Keywords: Lithium intercalation; Molybdenum oxide; Vanadium oxide

1. Introduction

The intercalation of a large amount of lithium into V_2O_5 leads to the formation, in the $Li_3V_2O_5$ composition, of the ω-type phase which exhibits a unique electrochemical behaviour in lithium batteries [1,2]. Most of the lithium atoms can be de-intercalated and then re-intercalated without important modification of this new in situ material formed. During the electrochemical cycling, up to 2.6 lithium atoms per V_2O_5 can be reversibly cycled in the 4 to 1.9 V range, leading to an experimental specific energy of V_2O_5 close to 900 Wh/kg. The X-ray characterization of this material shows that the structure can be considered as a derivative of the rocksalt structure, giving the $Li_xV_{0.4}O$ crystallographic formula. The limit compositions, which can be reached during the electrochemical cycling are therefore $Li_{0.6}V_{0.4}O$ and $Li_\epsilon\square_{0.6-\epsilon}V_{0.4}O$ in the discharged and charged state of the cell, respectively [3]. In the oxidized state, infrared and X-ray absorption spectroscopies show the formation of a short vanadyl-type bond, while, for the reduced material, the presence of a large amount of V^{3+} ions and the more homogeneous cationic charge distribution lead to a less-distorted lattice. When the ω-$Li_3V_2O_5$ phase is formed at the first discharge of the cell from the γ-$Li_xV_2O_5$ one, it exhibits a superstructure of the rocksalt lattice which leads to a tetragonal unit cell ($a = 9.23$ Å $c = 4.11$ Å) as clearly evidenced by an electron diffraction study realized by Weill et al. [4]. This superstructure may result from an ordered distribution of the vanadium ions which remembers that of the $Li_xV_2O_5$ precursor phases. At the first charge of the cell, when most of the lithium ions are removed, a structural reorganization occurs as suggested by a bump on the first galvanostatic charge curve or by a peak on the cyclic voltammogram. When the amount of lithium in $Li_xV_{0.4}O$ decreases, the rocksalt-type lattice becomes more and more unstable as a result of the increasing amount of cationic vacancies in the face-centred cubic (f.c.c.) oxygen packing; the observed structural reorganization results in a more homogeneous positive charge distribution, which stabilizes the material.

As reported by several authors, molybdenum can be substituted for vanadium in V_2O_5, leading to the $Mo_yV_{2-y}O_5$ solid solution ($0 \leqslant y \leqslant 0.60$) [5,6]. In this material, since the molybdenum ions stay at the hexavalent state, a corresponding amount of V^{4+} ions is present in order to maintain the overall charge balance. The presence of Mo^{6+} ions in the V_2O_5-type layer increases the three-dimensional character of the structure thanks to its stability in the octahedral en-

Elsevier Science S.A.
SSDI 0378-7753(94)02112-G

vironment. Several other phases with the general formula $Mo_{1+y}V_{2-y}O_8$ ($0 \leqslant y \leqslant 0.20$), exhibiting a structure strongly related to that of V_2O_5, have also been reported in the vanadium–molybdenum–oxygen system [7–9]. According to some results reported in the literature [8,10], and from our own experiences, it is very difficult to obtain the pure MoV_2O_8 end member phase; on the contrary, the $Mo_{1.2}V_{1.8}O_8$ phase ($Mo_6V_9O_{40}$) can easily be obtained.

Previous studies of the intercalation of lithium in some compositions of the $Mo_yV_{2-y}O_5$ solid solution ($0 \leqslant y \leqslant 0.60$) have been reported in the literature. Pistoia and co-workers [11,12] have studied particularly the behaviour of the $Li_xMo_{0.6}V_{1.4}O_5$ phase as the positive electrode for primary or secondary lithium batteries, while West et al. [13] reported the insertion of 1.5 lithium per transition element in these oxides. Although both research groups reported that irreversible structure modifications are observed upon cycling, no structural hypothesis has been done. Lithium has also been intercalated in both end members of the $Mo_{1+y}V_{2-y}O_8$ ($0 \leqslant y \leqslant 0.20$) solid solution [10,13–17]; all authors have reported irreversible structure modifications upon discharge, but not any characterization of the materials formed has been done, most of the reports claiming that an amorphous material was formed in such conditions.

In order to show that the formation of the ω-type phase is a general phenomenon in these oxide families, and to determine the effect of the vanadium oxidation state in the starting oxides on their redox potential versus lithium intercalation, chemical and electrochemical lithium intercalation studies in these materials have been performed. The first results are reported in this paper.

2. Experimental

The $Mo_yV_{2-y}O_5$ ($0 \leqslant y \leqslant 0.60$) phases are obtained by direct synthesis from the mixture of V_2O_5, V_2O_3 and MoO_3 oxides in stoichiometric proportions. The reaction, in a silica tube sealed under vacuum, requires two thermal treatments; 15 h at 500 °C and 70 h at 650 °C. The preparation of the $Mo_6V_9O_{40}$ phase is easier, as all cations being fully oxidized, the reaction can be realized under oxygen. Thus, the stoichiometric mixture of V_2O_5 and MoO_3 oxides is treated at 500 °C for 30 h and at 630 °C for 70 h.

The electrochemical lithium intercalation is realized in small laboratory cells with lithium as the negative plate, a solution of 1 M $LiClO_4$ in propylene carbonate as the electrolyte and a mixture of the studied material and Ketjen black (20 wt.%) as the positive electrode. These cells are cycled galvanostatically with a laboratory-made system built up around a HP 1000 minicomputer.

The chemical intercalation is done at room temperature with an excess of *n*-butyllithium with regard to the 1.5 lithium/transition element atomic ratio.

All these materials were chemically analyzed by inductively coupled plasma (ICP) spectrometry using the CNRS facilities.

3. Results and discussion

3.1. Starting phases

The X-ray diffraction (XRD) study of the $Mo_yV_{2-y}O_5$ ($0 \leqslant y \leqslant 0.60$) materials shows, in good agreement with previous results, the existence of a solid solution over the whole composition domain. For $y \leqslant 0.40$, these phases crystallize in the orthorhombic system like V_2O_5, while for $y = 0.60$ a small monoclinic distortion is observed. In all cases, the *c* parameter, that corresponds to the V–V intersheet distance, decreases continuously when molybdenum is substituted for vanadium; as a result of the stronger stability of hexavalent molybdenum in the octahedral than in pyramidal environment, the intersheet linking increases with *y*. The two-dimensional character of the V_2O_5 structure is well illustrated by its texture (thin platelets parallel to the sheets) as shown by a scanning electron microscopy (SEM) study. For the $Mo_yV_{2-y}O_5$ ($0 \leqslant y \leqslant 0.60$) phases, the SEM study points out that the thickness of the crystallites increases gradually with the amount of molybdenum. This evolution could result from the increasing three-dimensional character of the structure due to the presence of molybdenum in the octahedral environment. The idealized structures of these materials are represented in Fig. 1. While the square pyramidal environment of vanadium is used for V_2O_5 (Fig. 1(a)), an octahedral one has been assumed for the molybdenum-substituted phases (Fig. 1(b)). As it will be further discussed, this intersheet linking plays an important role during the lithium intercalation process.

In our study of the $Mo_{1+y}V_{2-y}O_8$ ($0 \leqslant y \leqslant 0.20$) solid solution, we did not succeed in obtaining the MoV_2O_8 phase; on the contrary, the $Mo_6V_9O_{40}$ phase has been obtained very easily. Its monoclinic unit cell parameters ($a = 19.38$ Å, $b = 3.625$ Å, $c = 4.124$ Å, $\beta = 90.7°$) are very close to those reported in the literature [9]. Ac-

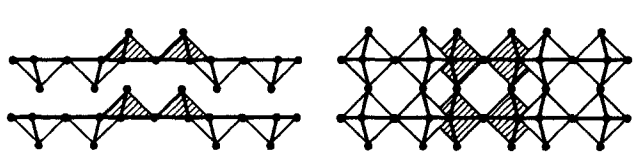

Fig. 1. Linking of the polyhedra in the V_2O_5-derived structures: (a) square pyramids description (V_2O_5), and (b) octahedra description ($Mo_yV_{2-y}O_5$).

cording to previous authors, the structure can be deduced, as shown in Fig. 2, from that of V_2O_5 by 'insertion' of an ReO_3-type file of octahedra (M1 sites) between two V_2O_5-type files of octahedra (M2 sites) (using the octahedral description of the V_2O_5 structure), the molybdenum atoms being preferentially situated in the M1 sites [16,18].

3.2. Electrochemical intercalation

Lithium has been electrochemically intercalated in the $Mo_yV_{2-y}O_5$ phases for $y=0.10$, 0.30, 0.40 and 0.60. The voltage limit in the discharge has been chosen smaller than 1.9 V in order to allow a deep discharge of the cell. The cycling curves obtained in such conditions are represented in Fig. 3 in comparison with those obtained for the unsubstituted V_2O_5.

In all cases, the ω-type phase is irreversibly formed at the end of the first discharge, as shown by the shape of cell voltage versus composition curve and confirmed by the XRD study of materials removed from the cells. In first approximation, the shapes of all cycling curves, relative to the ω-type phases, are nearly similar. There is no effect of the amount of molybdenum on the average cell voltage when the ω-type phase is formed. This fact, which is at first quite surprising since the substitution of molybdenum for vanadium requires a partial reduction of vanadium, will be discussed at the end of this paper.

On the contrary, the shape of the first discharge curves is very sensitive to the molybdenum amount. When it increases, the first part of the curve situated at high voltage, which corresponds to the reversible formation of the ϵ- and δ-$Li_xV_2O_5$ phases in the unsubstituted system, is considerably reduced and moreover the cell voltage decreases. An XRD study of these materials has shown that the linking between the sheets (due to the presence of molybdenum) makes it more and more difficult for the structural reorganisations to be observed with increasing x in the $Li_xV_2O_5$ system [19]. Therefore, the $\delta \rightarrow \gamma$ and $\epsilon \rightarrow \delta$ structural modifications are successively hindered with increasing y. Nevertheless, the ω-type phase is always obtained in the vicinity of the $Li_3Mo_yV_{2-y}O_5$ composition through a large potential plateau observed in the 2.2–2.4 V range. Simultaneously, the presence of an increasing amount of V^{4+} ions in the starting positive electrode material, when y increases, entails a gradual decrease in the cell voltage.

Like in the case of the ω-$Li_xV_2O_5$ system, there is a bump in the electrochemical curve during the first charge of the cell; it is well emphasized by the incremental capacity $-\Delta x/|\Delta V| = f(V)$ curve, represented in Fig. 4, for the $Li_xMo_{0.30}V_{1.70}O_5$ system. Such a behaviour, characteristic of an irreversible process, results from the disappearance of the superstructure which appeared when the ω-type phase was formed. This point will be discussed in detail in Section 3.3.

Medium-range cycling experiments have been performed in these materials. The average value of the

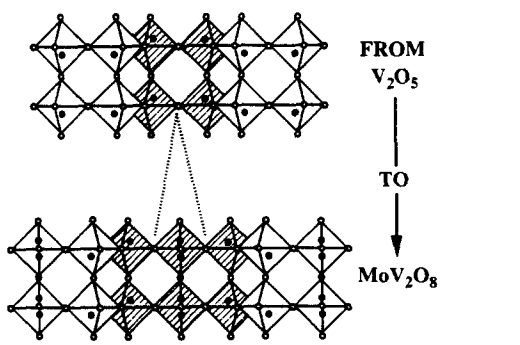

Fig. 2. Comparison between the polyhedra linking in V_2O_5 and in MoV_2O_8.

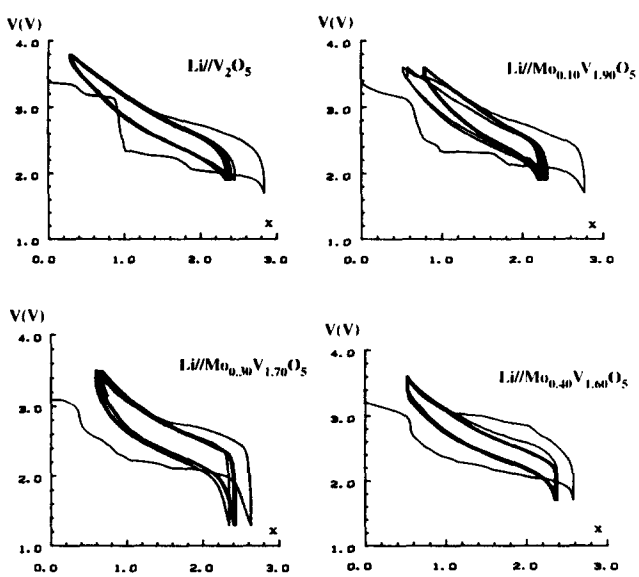

Fig. 3. First cycles of $Li/Mo_yV_{2-y}O_5$ cells showing the irreversible formation of the ω-$Li_3Mo_yV_{2-y}O_5$ phases, $y=0$, 0.1, 0.3, 0.4; $J=180$ $\mu A/cm^2$.

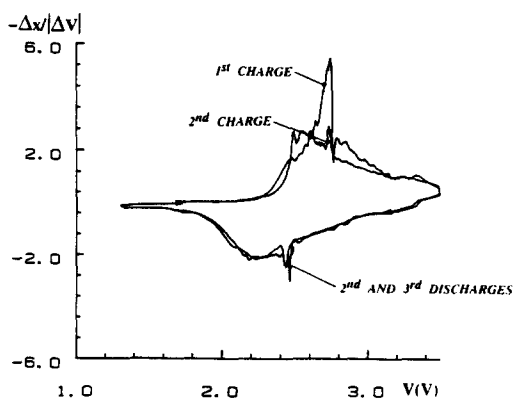

Fig. 4. Variation of incremental capacity vs. cell voltage for the first two cycles after the formation of the ω-$Li_xMo_{0.3}V_{1.7}O_5$ phase.

number of lithium atoms reversibly intercalated and de-intercalated per two transition elements and the specific energy are given in Table 1 for the various amounts of molybdenum. The number of intercalated/de-intercalated lithium is very close to that obtained for the unsubstituted material; nevertheless, the specific energy is significantly decreased as a result of the higher atomic weight of molybdenum versus vanadium.

Lithium has also been intercalated in $Mo_6V_9O_{40}$; in order to facilitate the comparison with previous results, the $Mo_{0.8}V_{1.2}O_{5.33}$-reduced formula with two transition elements has been used. The variation of cell voltage versus amount of intercalation is shown in Fig. 5. The shape of the cycling curve is very similar to the previous ones: the ω-type phase is formed at the end of the first discharge, the bump in the first charge curve characterizes a small structural reorganization. The variation of specific energy versus cycle number is reported in Fig. 6. The presence of a large amount of a heavy atom limits, also in this case, the specific energy. As an example, for a cycling in the 1.7–3.8 V range, the average specific energy for the first 12 cycles leads to 510 Wh/kg for $Mo_6V_9O_{40}$ against 790 Wh/kg for V_2O_5, although the numbers of exchanged lithium per transition element are very close (0.85).

3.3. Chemical intercalation

The ω-type phases have also been obtained by action of an excess of *n*-butyllithium on the $Mo_yV_{2-y}O_5$-mixed molybdenum–vanadium oxides. In all cases, the amount of lithium deduced from the chemical analysis is very close to 3. The XRD patterns of these materials are reported in Fig. 7 in comparison with those of ω-$Li_3V_2O_5$. Similarly to this phase, the XRD patterns have been indexed in the tetragonal system. The values of the unit cell parameters are summarized in Table 2. The main lines, that can be indexed in a cubic system, are characteristic of a rocksalt sublattice. The superstructure lines are more intense than in the unsubstituted material as a result of the high diffusion factor of molybdenum resulting from the high number of electrons. It is interesting to note that, in the case

Table 1
Variation of the average number of intercalated lithium (Δx) and of the average specific energy for the twelve first cycles

Molybdenum amount	Δx per transition element	Specific energy (Wh/kg)
0	0.990	790
0.10	0.740	600
0.30	0.870	570
0.40	0.900	620
0.60	0.850	540

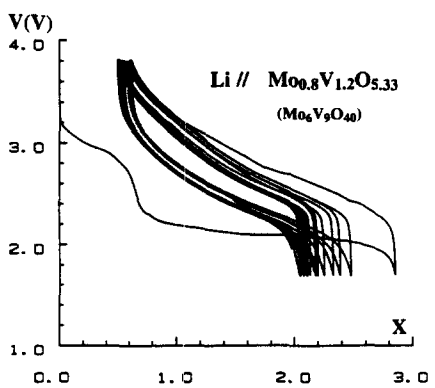

Fig. 5. First cycles of a Li/$Mo_{0.8}V_{1.2}O_{5.33}$ cell showing the irreversible formation of the ω-$Li_3Mo_{0.8}V_{1.2}O_{5.33}$ phase; $J = 180$ μA/cm^2.

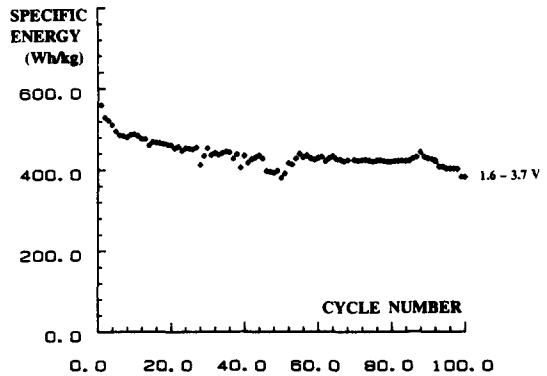

Fig. 6. Variation of cycle number vs. specific energy (per kg of the active positive electrode material) of an Li/$Mo_{0.8}V_{1.2}O_{5.33}$ cell cycled in the 3.7–1.6 V range.

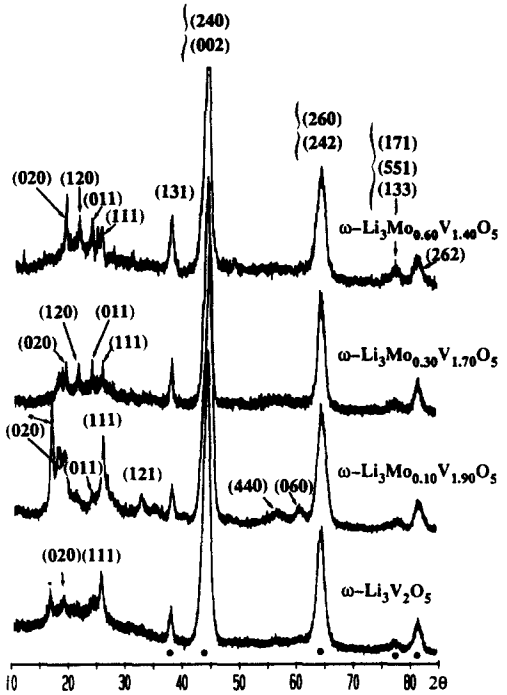

Fig. 7. X-ray diffraction patterns of the ω-$Li_3Mo_yV_{2-y}O_5$ phases, $y = 0$, 0.1, 0.3, 0.4. The X-ray diffraction lines which can be indexed in a cubic system are noted (•) in the case of the ω-$Li_3V_2O_5$ phase. The (*) corresponds to the strongest diffraction line of the γ-$Li_xV_2O_5$ phase.

Table 2
Tetragonal unit cell parameters of ω-$LiMo_yV_{2-y}O_5$ phases

Compound	a (Å)	c (Å)
ω-$Li_3V_2O_5$	9.23	4.11
ω-$Li_3Mo_{0.1}V_{1.9}O_5$	9.26	4.01
ω-$Li_3Mo_{0.3}V_{1.7}O_5$	9.25	4.05
ω-$Li_3Mo_{0.6}V_{1.4}O_5$	9.23	4.07

of V_2O_5 or slightly molybdenum-substituted materials, the superstructure of the ω-type phase is formed by intercalation in the γ-phase. On the contrary, when the molybdenum-substitution amount increases, it is formed by intercalation in the δ- and even ϵ-phase during the first cell discharge.

These materials have been used as the positive electrode of lithium batteries. The shape of the charge/discharge curves is similar to that obtained when the ω-type phase is formed in situ within the electrochemical cell. On cycling, the superstructure lines disappear and only the cubic lines remain. Therefore, the crystallographic formula of the ω-type phase is $Li_x\square_{0.60-x}Mo_v$-$V_{0.40-v}O$ with $v=y/5$.

All these materials have been characterized by X-ray absorption (XANES and EXAFS) in collaboration with Fargin [19]. The evolution of the Mo-O and V-O distances, as well as that of the polyhedra distortion versus the amount of lithium and molybdenum shows that: (i) the reduction of molybdenum to the pentavalent state occurs after complete reduction of vanadium to the tetravalent state; (ii) pentavalent molybdenum tends to form a short molybdenyl-type bond, and (iii) the presence of a large amount of trivalent vanadium tends to prevent any polyhedra distortion.

4. Conclusions

The formation of ω-type phases by intercalation of a large amount of lithium in V_2O_5-derived material is a very general phenomenon since it does occur in molybdenum-substituted materials like $Mo_yV_{2-y}O_5$ and even $Mo_6V_9O_{40}$. The structure of the ω-type phase can be described from an f.c.c. oxygen array with cations statistically distributed in the octahedral sites of the rocksalt structure. When this phase is formed for the first time, a superstructure, characterized by a tetragonal unit cell, is obtained. It disappears during the first lithium de-intercalation thanks to the cation redistribution which occurs to minimize the electrostatic repulsions in the highly deficient rocksalt structure obtained upon intercalation. For all materials, the shape of the electrochemical cycling curves are almost similar, independently of the molybdenum amount. There is no effect of the presence of an increasing concentration of tetravalent vanadium in the starting $Li_xMo_yV_{2-y}O_5$ phase on the cell voltage. This result shows clearly that the rapid increase in the cell voltage at the end of the de-intercalation results rather from the difficulty to remove lithium ions from a highly deficient phase than from the intrinsic cation-oxidizing character.

Acknowledgements

The authors wish to thank ADEME and CNES for financial support, M. Ménétrier for fruitful discussions, S. Brèthes and C. Denage for technical assistance.

References

[1] C. Delmas, S. Brèthes and M. Ménétrier, *J. Power Sources, 34* (1991) 113.
[2] C. Delmas, A. Levasseur, M. Ménétrier and S. Brèthes, *Eur. Patent No. 909 055 550.*
[3] H. Cognac-Auradou and C. Delmas, *Solid State Ionics,* submitted for publication.
[4] F. Weill, H. Cognac-Auradou and C. Delmas, *J. Solid State Chem.,* submitted for publication.
[5] L. Kihlborg, *Acta Chem. Scand., 21* (1967) 2495.
[6] J. Darriet, *Thesis,* University of Bordeaux I, France, 1971.
[7] A. Magneli and B. Blomberg, *Acta Chem. Scand., 5* (1951) 585.
[8] H.A. Eick and L. Kihlborg, *Acta Chem. Scand., 20* (1966) 1658.
[9] R.C.T. Slade, A. Ramanan, B.C. West and E. Prince, *J. Solid State Chem., 82* (1989) 65.
[10] A. Tranchant and R. Messina, *J. Power Sources, 24* (1988) 85.
[11] P. Fiordiponti, M. Pasquali, G. Pistoia and F. Rodante, *J. Power Sources, 7* (1981–82) 133.
[12] M. Pasquali, G. Pistoia and F. Rodante, *J. Power Sources, 7* (1981–82) 145.
[13] K. West, B. Zachau-Christiansen, S. Skaarup and T. Jacobsen, *Solid State Ionics, 53–56* (1992) 356.
[14] J. Labat, V. Dechenaux, Y. Jumel and J.P. Gabano, *Proc. Meet. The Electrochemical Society,* Proc. Vol. 88–6, 1988, p. 494.
[15] Y. Muranushi, T. Miura, T. Kishi and T. Nagai, *J. Power Sources, 20* (1987) 187.
[16] Y. Takeda, R. Kanno, T. Tanaka and O. Yamamoto, *J. Electrochem. Soc., 134* (1987) 641.
[17] M. Uchiyama, S. Slane, E. Plichta and M. Salomon, *J. Electrochem. Soc., 136* (1989) 36.
[18] R.H. Jarman, P.G. Dickens and A.J. Jacobson, *Mater. Res. Bull., 17* (1982) 325.
[19] H. Cognac-Auradou, *Thesis,* University of Bordeaux I, France, 1993.